# Fatigue resistance of low pressure nitrided Cr-Mo low alloy steels

D. Firrao, G. Ubertalli, E. Morgano, A. Brunelli

Fatigue resistance of steel parts can be improved by nitriding, the more the deeper is the layer affected by nitrogen diffusion, as stated by the Lessells-Firrao law. Low-pressure nitriding has been applied to wheel's hubs fabricated with a quenched and tempered Cr-Mo low alloy steel. N diffusion depths have been compared to similar results obtained with the same type of automotive parts subjected to classical gas nitriding. 12 h total low-pressure treatment time provided an almost 100% increase of hardened depth over 40 h gas nitrided parts. Both treatments allowed reaching an adequate fatigue life, whereas induction hardened parts did not. X-ray diffraction analysis provided phase constitution of top converted layers in both nitriding cases. A rationale based on the effect of early treatment stage top layer formation has been developed.

**KEYWORDS:** NITRIDING; LOW PRESSURE NITRIDING; FATIGUE RESISTANCE; X-RAY DIFFRACTION; DIFFUSION DEPTHS;

## INTRODUCTION

The thermochemical treatment of nitriding or nitrocarburizing allows to obtain on the steel surface the formation of a thin surface layer, where γ'-$Fe_4N$ nitrides or crystals of the ε-solid solutions of the C-Fe-N system predominate. Both of these phases are characterized by slight or much higher hardness values as compared to the material that is subjected to nitrogen enrichment treatment. A thicker nitrogen diffusion layer with the precipitation of carbides or nitrides of various types follows.

The formation of nitrides and carbonitrides occurs as a result of nitrogen enrichment of the steel original constituents, mainly ferrite and cementite (taking into account the metastable ternary phase diagram, Fig. 1), which, by reaching the saturation limit, cause phase changes in the material.

The surface enrichment of atomic nitrogen and the formation of these new phases leads to atomic enrichment and to a situation of atomic compression that generates negative residual stresses in the surface layers of the material, whose origin has been attributed to volume changes (precipitation and content evolutions) and thermal effects [1,2,3]. However, the mechanical components do not show substantial overall dimensional changes and do not require grinding subsequent to surface treatments.

D. Firrao, G. Ubertalli
DISAT, Politecnico di Torino, Torino

E. Morgano
Centro Ricerche Fiat, Torino, (ora Silco Srl, Rivalta (TO))

A. Brunelli
Tra.Ind Srl, Nichelino (TO)

After the nitriding or nitrocarburizing treatment, the material shows a high surface hardness, a low tendency to scratch, a high resistance to wear, an increase in the fatigue limit and a good corrosion resistance in atmospheric, pure water and steam environments [4,5,6].
The increase in fatigue strength of the nitrided components is described by the following Lessells-Firrao law [7],

$$\sigma_{d,t} = 1.25 \cdot \sigma_{d,nt} \cdot {}^{D}/_{(D-2d)} \quad (1)$$

$\sigma_{d,t}$ and $\sigma_{d,nt}$ represent the endurance limits under rotating bending for treated and untreated steel bars, respectively; $D$ is the bar diameter and $d$ the nitrogen diffusion layer thickness, respectively.
This relationship highlights that the deeper is the layer affected by nitrogen diffusion (d), the greater the fatigue strength ($\sigma_{d,t}$).

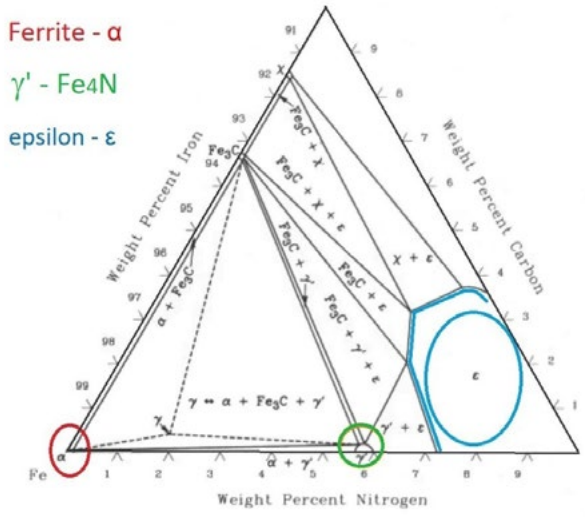


**Fig.1** - Metastable Fe-C-N diagram isothermal section at 565 °C [8]. In the evidenced colored areas, there are shown the fields of existence of the ferrite, $Fe_4N$-γ' and epsilon phases respectively.

To provide nitrogen to the steel surface by a gaseous environment, the use of ammonia is necessary, by the following dissociation reaction (catalysed by Fe itself):

$$NH_3 \leftrightarrow N_{(in\ \alpha-Fe)} + {}^{3}/_{2}\, H_2 \quad (2)$$

When N saturates α-Fe, the following successive reactions set in:

$$NH_3 + \alpha \leftrightarrow Fe_4N + {}^{3}/_{2}\, H_2 \quad (3)$$

$$NH_3 + Fe_4N \leftrightarrow \varepsilon + {}^{3}/_{2}\, H_2 \quad (4)$$

All the three reactions yield the same formal expression for the nitrogen activity $a$(N),

$$a(N) = const \cdot \frac{P_{NH_3}}{(P_{H_2})^{3/2}} = const \cdot K_N \quad (5)$$

where obviously the constant varies with the reaction and the temperature; the nitrogen activity refers to the specific phase that is considered in the reactions (2, 3 or 4). The ratio $P_{NH3}/P_{H2}^{3/2}$ is often referred to as the nitriding potential and it is indicated as $K_N$. The nitrogen activity, $a$(N), is first-order proportional to the ammonia partial pressure. By writing Eq. 5 in terms of molar fractions, the following equation is obtained

$$a(N) = const \cdot \frac{y_{NH_3}}{(y_{H_2})^{3/2}} \cdot \frac{1}{\sqrt{P}} \quad (6)$$

Eq. 6 shows that, by reducing the overall pressure ($P$), the nitrogen activity of the solids is increased, as well as the nitriding potential [9]; the equilibrium goes towards a higher nitrogen activity, i.e. a greater content of the nitrogen in the formed phases, especially in case of the **ε** solid solution, which has the largest field of stability.
Furthermore, by lowering the pressure, the diffusion kinetics in the gaseous phase layer in contact with the surface of the components increase, because the thickness of the gaseous boundary layer increases, favoring mass transport and leading to an increase in the deposition rate. [10]

## EXPERIMENTAL

Wheel hubs of extensive production for the automotive field (Figs. 2 and 3 show the axonometric view and the real image of the component), fabricated with 42CrMo4 (EN ISO 683-2:2016) low alloy steel, roughly corresponding to SAE 4140, have been subjected to three different surface hardening treatments. All the mechanical components had previously been quenched and tempered at 600°C.
In particular, a first group of components was subjected to induction surface hardening, followed by low temperature tempering and shot peening in a specific area, highlighted in Fig. 3 with a yellow line (required hardness > 52 HRC). This is the area subjected to fatigue failure in case of the usual operating conditions of the wheel hubs.
A second group of components taken from the same batch was subjected to a gaseous 1 bar nitriding treatment with a two-stages process: a first stage at 510 °C for 20 h and with nitriding potential $K_N$ = 2.97 and a second one at 530 °C for 20 h and with a nitriding potential of $K_N$ = 0.77.
A third one was subjected to a low-pressure nitriding treatment with a cycle with a first step at 520 °C for 6 h and with $K_N$ = 4.8; in the second step the temperature was 550 °C with $K_N$ = 0.79. The total process duration was 15 h at pressures that varied from 0.3 to 0.8 bar during the process.

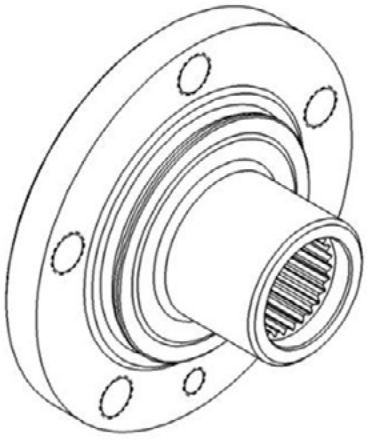

**Fig.2** - 3D view of the wheel's hub.

**Fig.3** - Real image of the wheel's hub after nitriding and sample cutting for metallographic analysis. The yellow line shows the notch area subjected to induction hardening and shot peening.

Taking into consideration the $K_N$ nitriding potential of the conventional treatment at 1 bar, it is possible to position the working conditions for the first stage (•) and for the second stage (*) on the Lehrer diagram [11] which represents, for different degrees of dissociation of the ammonia (different $NH_3/H_2$ ratios), the thermodynamic conditions among the $NH_3$ e $H_2$mixtures, the treatment temperatures and the phases in equilibrium.

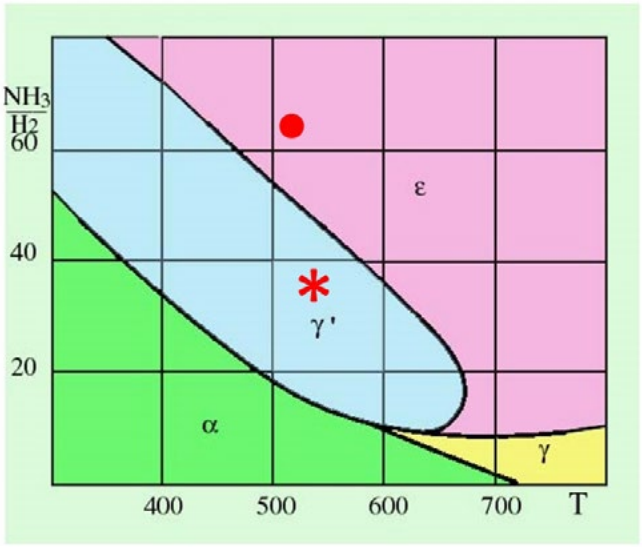


**Fig.4** - Lehrer diagram for $NH_3$ - $H_2$ gas mixtures in equilibrium with solids of the Fe-N system (*P* = 1 bar). On the diagram the nitriding potential conditions for the first (•) and second (*) stage in case of conventional nitriding treatment are reported.

The wheel hubs were analyzed by the Optical Emission Spectrometer (OES) - GNR—MetalLab32; in Table1 the chemical composition of the wheel hubs is reported. The results confirm that the steel is a 42CrMo4.

**Tab.1** - Chemical composition of the 42CrMo4 Steel (mass pct.)

| 42CrMo4 | C | Si | Mn | Mo | Cr | Fe |
|---|---|---|---|---|---|---|
| | 0.43 | 0.27 | 0.82 | 0.21 | 1.03 | bal. |

After the three surface hardening treatments, the wheel's hubs underwent rotating bending fatigue tests, with both constant radial (1055 daN) and axial loads (844 daN). Endurance up to 600,000 cycles was considered successful.
Wheel's hubs subjected to conventional or low-pressure nitriding treatments passed the fatigue limit test of 600,000 cycles, whereas most of the locally hardened induction hardened, stress relieved and shot peened hubs failed before the 600,000 cycle limit exactly at the hardened notch marked with a yellow line in Fig. 3.
Given the results obtained from the fatigue tests, in order to better understand the constitution of the surface hardened layers, some samples of the wheel hubs, subjected to conventional or low-pressure nitriding treatments, were subjected to metallographic and hardness analysis, as well as roentgenographic tests by a Rigaku D-MAX III diffractometer equipped with Co anode, $K_{\alpha 1}$ = 0.178899 nm, and with carbon monochromator.
The metallographic observations carried out on the polished and etched transverse sections of the samples allowed to highlight the presence, for both nitriding treatments, of a homogeneous white layer – Fig. 5 -, which was found to be 12-14 μm deep with a porosity of about 50% (Table 2). Below this layer, a thicker nitrogen diffusion layer can be observed- Fig. 6.

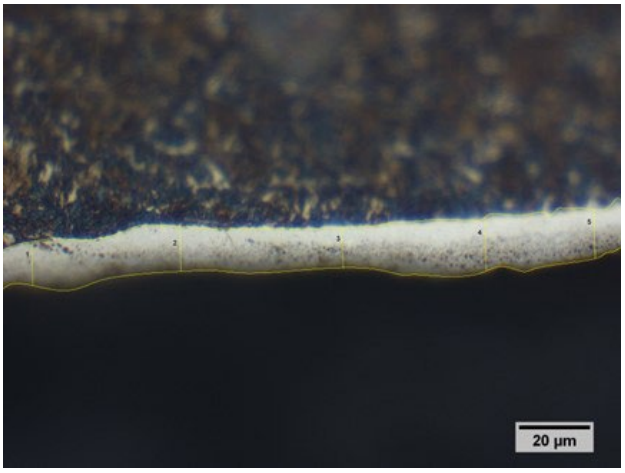


**Fig.5** - Metallographic image of the white layer of a low-pressure nitrided hub.

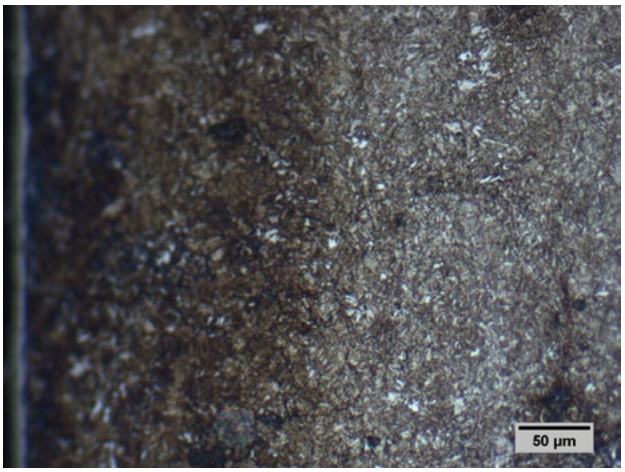


**Fig.6** - Metallographic image of the diffusion layer of a low-pressure nitrided hub.

**Tab.2** - Surface and core hardness, effective hardening depth and white layer thickness with porosity percentage after nitriding processes.

| Nitriding | Surface hardness [HV 1] | Core hardness [HV 10] | Effective depth [mm] | Top layer depth [µm] |
|---|---|---|---|---|
| Low pressure | 732 - 752 | 298 - 302 | **0.45** | 12 - 14 (50% porous) |
| Conventional | 650 - 672 | 298 - 302 | **0.27** | 12 – 14 (50% porous) |

The hardness tests, carried out on the surface (load 1 kg) and at the core (load 10 kg), show that the low-pressure nitriding treatment yields higher surface hardness values (about 80 HV1 points) than the conventional one.
Microhardness test profiles with 100 g load were carried out on the transverse section of metallographic samples, what allowed to evaluate the effective hardening depth, determined at 100 HV more than the core hardness – Fig. 7.

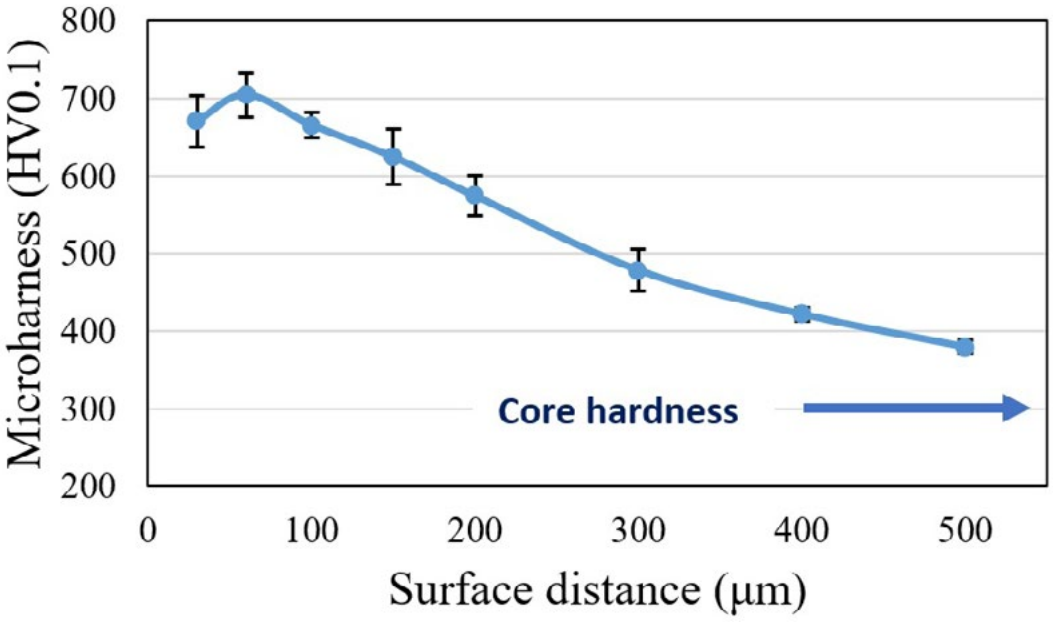


**Fig.7** - Low pressure nitriding microhardness profile and standard deviation ranges (HV 0.1).

The wheel hubs, atmospheric and low-pressure nitrided, were analyzed by X-ray diffractometric methods to evaluate the constitution of the phases in the surface layers. The peaks of the ε phase and of the γ′ phase in the white layer and that of the α-ferrite peaks, present in the diffusion layer, were detected, confirming the modest thickness of the top layer, Fig. 8.

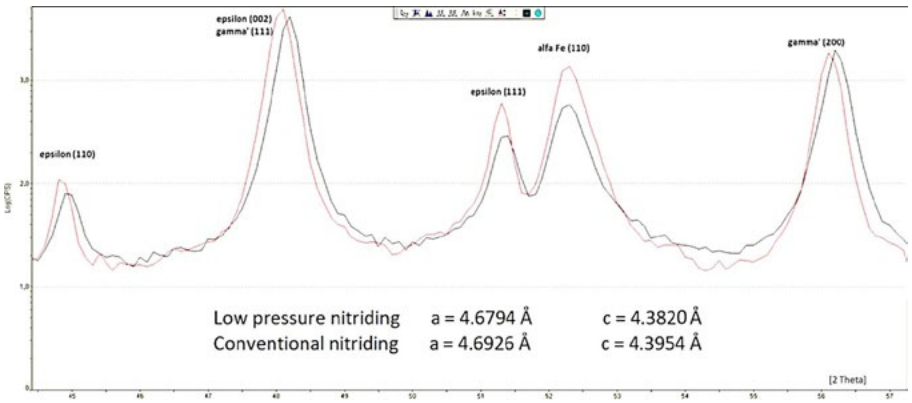


**Fig.8** -X-ray diffraction spectra of low-pressure (------ black line) and conventionally (------ red line) nitrided samples. Below the background, the derived cell parameters of the ε-phases are reported.

The quantitative evaluations of the percentage of the three phases in the layers were carried out by measuring the areas underlying the roentgenographic peaks and by comparing them with the values obtained with mixtures of powders used as standards. In the case of hubs subjected to low pressure nitriding, it was possible to quantify as 17% the amount of the ε phase, as 60% that of γ'-$Fe_4N$ and as 23% that of α-ferrite present in the substrate. In the case of the conventional nitriding treatment, the quantitative analysis shows 21% of the ε phase, 52% of γ'-$Fe_4N$, and 27% of α-ferrite. The higher γ'-$Fe_4N$ phase content in the surface layer in case of the low-pressure nitriding treatment is also reflected by the higher surface hardness obtained.

From the positions of the peaks of the ε phases, the lattice constants a and c of the hexagonal cell were computed. The hexagonal lattice parameters result slightly smaller in

the case of the low-pressure nitriding treatment, as reported in Fig. 8.

By using the diagram of Fig. 9, it was possible to derive the atomic interstitial content (C+N) in the epsilon phases for both treatments, obtaining values of 25.2% in the case of low-pressure nitriding, and 25.7% in the conventional one.

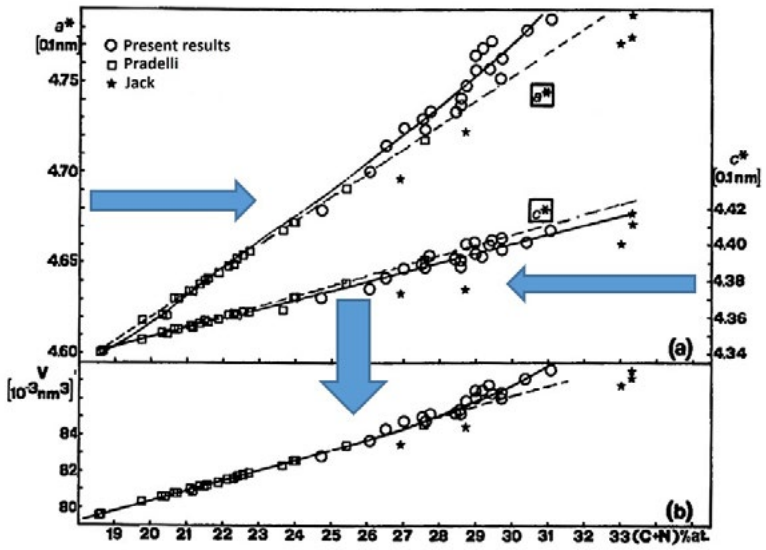


**Fig.9** -Graph reporting the relation between the (C+N) at % content and the hexagonal lattice parameters of ε phases [12].

Assuming that the C content in the ε phase is the same for both the treatments, it follows that the nitrogen content is lower in the case of the low-pressure treatment, which reflects a higher temperature last stage (Fig. 10).

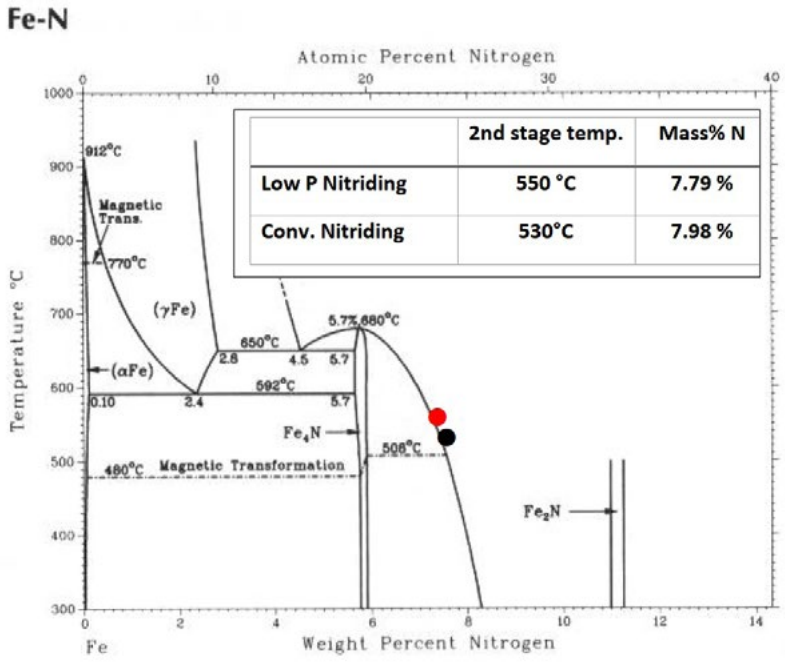


**Fig.10** -Metastable Fe-N phase diagram and the mentioned nitrogen concentration for low-pressure (●) and conventional (●) treatments.

## CONCLUSIONS

The most important findings of the experimental work on surface hardening treatments, carried out on 42CrMo4 steel (AISI 4140 steel) wheel hubs for automotive use, can be summarized as follows:

Both the thermochemical treatments have made possible to obtain a fatigue life exceeding the prescription of 600,000 cycles, unlike the induction hardening plus shot peening treatment.

The low-pressure nitriding treatment allowed the formation of a hardened surface layer with a greater hardness of about 80 HV1 points, with a nitriding treatment time of only 15 h, compared to 40 h of the conventional nitriding treatment.

Finally, the actual depth of hardening, measured with the conventional hardness of 100 HV points higher than that of the component core one, shows an almost double thickness, reaching 0.45 mm. By the Lessells-Firrao law, it indicates that the low-pressure fatigue endurance can be much higher than the one pertaining to conventional 1 bar nitriding.

## REFERENCES

[1] L. Barrallier, J. Barrallis: Proceedings of ICRS4 (1994), 498-505.
[2] H. Oettel, G. Schreiber: AWT-Tagungsband, Wiesbaden, Germany (1991), 139-151.
[3] E.J. Mittemeijer, A.B.P. Vogels, P.J. van der Schaaf: J Mater Sci, Vol. 3 (1980), 153.
[4] H.C.F. Rozendaal, P.F. Colijn, E.J. Mittemeijer: Surf Eng, Vol. 5 (1985), 30.
[5] E.J. Mittemeijer: J Heat Treat, Vol. 3 (1983), 114.
[6] E.J. Mittemeijer: Mater Sci Forum, Vol. 223 (1992), 102-104.
[7] D. Firrao, D. Ugues, Mat. Sc. And Eng. A, Vol. 409 (2005), 309-316.
[8] ASM Handbook: Alloy Phase Diagram - Editor: George F. Vander Voort – ASM International -Volume 3 (2004).
[9] D. Jordan, H. Antes, V. Osterman, T. Jones, Vacuum nitriding of 4140 steel, Heat. Treat. Prog. Vol. 3–4 (2008), 33–38.
[10] Wolowiec-Korecka, Michalski, Kucharska, Kinetic aspects of low-pressure nitriding process, Vacuum Vol. 155 (2018), 292-299.
[11] E. Lehrer, Zeitschrift fuer Elektrochemie und Angewandte Physikalische Chemie Vol. 36, (1930), 383.
[12] A. BURDESE, D. FIRRAO, M. ROSSO, Gazz. Chim. Ital., Vol. 113 (1983), 265-268.

# Resistenza a fatica di acciai basso legati al Cr-Mo nitrurati a bassa pressione

La resistenza a fatica dei componenti in acciaio può essere migliorata con il trattamento di nitrurazione, in entità tanto maggiore quanto più profondo è lo strato interessato dalla diffusione dell'azoto, come stabilito dalla legge di Lessell-Firrao. La nitrurazione a bassa pressione è stata applicata a mozzi di ruote fabbricati con un acciaio a bassolegato al Cr-Mo bonificato. Le profondità di diffusione dell'azoto sono state confrontate con quelle ottenute sullo stesso tipo di parti automobilistiche soggette alla classica nitrurazione a gas. Il tempo totale di trattamento a bassa pressione, di 12 ore, ha fornito un aumento di quasi il 100% della profondità indurita, rispetto alle 40 ore richieste per le parti nitrurate a gas. Entrambi i trattamenti hanno consentito di raggiungere un'adeguata durata a fatica, mentre i pezzi temprati ad induzione no. L'analisi della diffrazione dei raggi X ha fornito la costituzione degli strati superiori formatisi in entrambi i casi di nitrurazione. È stata illustrata la logica basata sull'effetto della formazione dello strato superiore nella fase iniziale del trattamento.

**PAROLE CHIAVE:** NITRURAZIONE, NITRURAZIONE A BASSA PRESSIONE, RESISTENZA A FATICA, DIFFRAZIONE, PROFONDITÀ DI DIFFUSIONE;

TORNA ALL'INDICE >